Military Technical College
Kobry El-Kobbah,
Cairo, Egypt.

13th International Conference on Applied Mechanics and Mechanical Engineering.

THE HEAT DEFORMATION ANALYSIS IN BRIDGE CARRIER

TAECHAJEDCADARUNGSRI S.[*,**], SAENSUMRONG K.[***],
and HORMDEE D.[*,****]

ABSTRACT

Bar lapping is a key process in Slider Micro-Fabrication Process of Hard Disk Drive (HDD) industry. The purpose this process is to remove a small amount of material so that the transducer Sensor Height (SH) variation across the bar is minimized. One of the main problems occurred during the lapping process is bar bowing, which damages both ends of slider bar causing the difficulty to control SH. In this study, the commercial ANSYS software is employed to evaluate the bar bowing profiles before and after the design improvement. Before the lapping process, the slider bar needs to be mounted on a bridge carrier with the wafer gripper, which functions as an adhesive between these two parts. The bridge carrier with wafer gripper and bar is then heated up in an oven in order to melt the adhesive for the bonding process. In this process, the bridge carrier is expanded and consequently causes the bar bow problem. In order to solve the problem, the stainless bar is inserted into the bridge carrier for the reinforcement. The results from the finite element model show that the deflection of the bar is reduced by 38%. The actual data of bar bow profile before the reinforcement is measured from the field. The results are similar to the profiles simulated via FEM. As a result, the conclusions from FEM could be applied as a guideline to the new bar lapping development.

KEY WORDS

Lapping Process, Slider, Slider Bar, Bridge Carrier and Sensor Height

* Researcher, Industry/University Cooperative Research Center (I/UCRC) in HDD Component, Khon Kaen University, Khon Kaen 40002, Thailand.

** Assistant Professor, Dpt. of Mechanical Engineering, Khon Kaen University, Khon Kaen 40002, Thailand. (Corresponding Author: sirtae@kku.ac.th)

*** Graduate student, Dpt. of Mechanical Engineering, Khon Kaen University, Khon Kaen 40002, Thailand.

**** Assistant Professor, Dpt. of Computer Engineering, Khon Kaen University, Khon Kaen 40002, Thailand.

INTRODUCTION

Arial Density has been drastically increased in current Hard Disk Drive (HDD) industry. This also yields to decreasing slider's fly height or; in other words, improving the effectiveness of magnetic field's reading/writing. Therefore, the control of sliding bar shape is the key that affects the flying. One of the bulging adjustment processes is Lapping Process, which opens recording head sensor. This process depends on the fixed size of Sensor Height (SH). This SH, illustrated in Fig. 1, is the important distance for data recording; hence, the control of it is also very essential.

Lapping Process (Fig. 2) starts from taking a bar cut from a wafer consisting of approximately 20-50 reading heads or more. The height of the SH can be calculated from values read from Lap resistance sensor or from ELGs (Electrical Lapping Guide) which estimates the SH. In the lapping process, the SH can be varied from 0.1 to 10 micrometers.

According to the above explanation, it is difficult to control the lapping process when the slider bar is bowed. A factor that also causes slider bar to be bowed is the heat used to melt the glue to hold carrier and slider bar together. This is because in order to melt the glue, the temperature has to be between 100 to 150^{o}C, which is also high enough to cause heat deformation in bridge carrier, hence, the bowing slider bar. Even though the deflection of slider bar bowing occurs in a small scale, it is relatively important enough compared to SH range. The part that causes bar bowing is the deflection of the bridge carrier's fingers, depicted in Fig. 3. Therefore, slider bar bowing can be lessened by temporally reinforcing old structure with stronger equipment.

BRIDGE CARRIER

The bridge carrier has three main parts: firstly, the Base that helps hold together the fingers, secondly, Fingers, the key parts controlling SH range in lapping process, and lastly, the Cover, that holds the base and fingers together ready to be assembled with automatic bar lapping machine.

Finger Model

Figure 3 illustrates a model of the fingers, which consists of four materials that are bonded together. The comparison between the fingers with and without metal bar before they are heated is shown in Fig. 4.

Properties of Materials in Fingers

The whole structure of fingers consists of

- Fingers Structure, made of 400 stainless steel,
- Axis, made of 400 stainless steel,
- Slider Bar, made of Al2o3-TioC Composites,
- Metal bar, made of 300 stainless steel. All materials have Isotropic properties constraints as shown in Table 1.

THEORIES

According to stress and strain relations of linear materials, it can be explained by equation 1. [1]

$$\{\sigma\} = [D]\{\varepsilon^{el}\} \tag{1}$$

$\{\sigma\}$ = Stress vector = $[\sigma_x\ \sigma_y\ \sigma_z\ \sigma_{xy}\ \sigma_{yz}\ \sigma_{xz}]^T$, $[D]$ = elastic stiffness matrix and $\{\varepsilon^{el}\} = \{\varepsilon\} - \{\varepsilon^{th}\}$ = elastic strain vector) then $\{\varepsilon\}$ = $[\varepsilon_x\ \varepsilon_y\ \varepsilon_z\ \varepsilon_{xy}\ \varepsilon_{yz}\ \varepsilon_{xz}]$ and $\{\varepsilon^{th}\}$ = thermal strain vector.

According to equation 1, the strain relations can be explained by the following equation:

$$\{\varepsilon\} = \{\varepsilon^{th}\} + [D]^{-1}\{\sigma\} \tag{2}$$

Since it is 3-dimention problem analyses, the equation is

$$\{\varepsilon^{th}\} = \Delta T[\alpha_x^{se}\ \alpha_y^{se}\ \alpha_z^{se}\ 0\ \ 0\ \ 0]^T \tag{3}$$

α_x^{se} is Secent coefficient of thermal expansion, $\Delta T = T - T_{ref}$ when T is temperature of interest, and T_{ref} is reference temperature of the material that is not deformed yet, and $[D]^{-1}$ is flexible or compliance matrix.

$$[D]^{-1} = \begin{bmatrix} 1/E_x & -\nu_{xy}/E_x & -\nu_{xz}/E_x & 0 & 0 & 0 \\ -\nu_{yx}/E_y & 1/E_y & -\nu_{yz}/E_y & 0 & 0 & 0 \\ -\nu_{zx}/E_z & -\nu_{zy}/E_y & 1/E_y & 0 & 0 & 0 \\ 0 & 0 & 0 & 1/G_{xy} & 0 & 0 \\ 0 & 0 & 0 & 0 & 1/G_{yz} & 0 \\ 0 & 0 & 0 & 0 & 0 & 1/G_{xz} \end{bmatrix}$$

FINITE ELEMENT METHOD

Constraints

According to the finger model, the boundary conditions are as follows:
- Reference temperature is 25°C or 298 K;
- Current temperature, constant temperature on the outer surface, is 130°C or 403 K;
- Degree of freedom at surface between fingers and base is zero as shown in Fig.5.;
- Finger surface and axis are bonded;

- Supposed that the slider bar surface and fingers are bonded regardless of glue in between because this is tendency-comparing analysis in order to adjust bowing;
- Metal bar is bonded to fingers and is linear material;

Results of Finite Element Method

Figures 6 and 7 show the deformation of fingers when heated according to the defined boundary condition. The area of interest is the surface's front edge because it is where SH in the slider bar with 30 - 50 lap sensors needing to be controlled so that slider bar is covered. There are 46 sensors in Finite Element Method so that there is bulging range and average figure of each slider. Then, bulging figure is compared with the bridge carrier with metal bar by using the same method.

The result of the model via Finite Element Method in Fig. 8 shows that adding a metal bar lessen the bar bulging by 38%. Or it can be said that the slider bar plane is more even with this approach.

EXPERIMENTAL RESULT

After heated and cooled down 2059 slider bar samplings, the measurements via image processing from the bar bow machine of 8 locations along the bar yield to the average bar curve plotted in Fig. 9. Bridge carriers that have been functioned after about 180-2160 life cycles, or 1-12 months of their usages cause this bar curve.

Though the results from FEM are not the real measured data, with the similar boundary conditions, the results from FEM and the actual measurement can be used together to tell a story here. Figure 10 shows the bar curve results from FEM along with the data from the actual measurement and also the results from FEM simulated after metal bar insertion. The last case is a showcase where FEM comes in useful. The graph illustrates that adding stainless bar helps make the surface of the slider bar more even.

Bridge carriers used in the experiment are divided into two groups: Control and Evaluation groups, with 46 points of the bars' surface plains measured by Coordinate Measuring Machine (CMM). Bar bowing profile before and after heated in the oven are measured in both groups. The difference is stainless bar is inserted in the Evaluation group during the heating process. Figures 11 and 12 show the comparison of the results before and after of the Control and Evaluation groups respectively.

From those two graphs, the gaps between before and after heated cases for both groups seem to be negligible. However, considered Fig. 13 which depicts the differences between before and after heated for both groups in finer resolution, the graph shows that bar deformation trend of the Control group (opaque line) remains steady whilst of the Evaluation group (dashed line) with stainless bars in bridge carriers appears to bend down. This can be concluded that stainless bars help reduce the bowing in the already-bow-bridge carriers.

CONCLUSIONS

The results from the Finite Element Model (FEM) show that the deflection of the bar is reduced by approximately 38%. The actual data of bar bow profile before the reinforcement is measured from the field. The results are similar to the profiles simulated via FEM. This can also be said that the proposed approach, by inserting metal bar, smoothens the surface of slider bars. Due to the limitation of the on-site measuring machine, the accessible of lapping machines, and the expense of the high-end machine tools, only a few samples of the bridge carriers with and without the metal bar reinforcement were built and used in the actual lapping process in order to verify with the numerical results. From the experiments, the bridge carriers expand after some cycles of their usages and start to show the bar bowing profiles. The measuring results show that the bridge carriers with the metal bar reinforcement give better curvature of bar bowing profile.

ACKNOWLEDGEMENT

This research is supported by Seagate Technology (Thailand). Kriengsak Saensumrong is funded by Changpeuk Modindaeng Scholarship, the Faculty of Engineering, Khon Kaen University, Thailand.

REFERENCES

[1] Chandrupatla, T.R. and Belegundu, A.D., Finite Elements in Engineering, Prentice-Hall, Upper Saddle River, New Jersey (1997).
[2] Gatzen, H.H., Maetzig, J.C. and Schwabe, M.K., “Precision Machining of Rigid Disk Head Sliders”, *IEEE Trans. Magn*., 23 (3), pp. 1843-1849 (1996).
[3] Howard E.B. and Timothy L.G., Eds., “Metals Handbook”, *American Society for Metals, Materials Park*, OH (1985).
[4] Jiang, M., Hao, S., and Komanduri, R., “On the advanced lapping process in the precision finishing of thin-film magnetic recording heads for rigid disc drives”, *Springer-Verlag*, vol.77, pp.923-932, Dec (2003).
[5] Mei, Y. and Stelson, K.A., “Lapping Control of hard disk drive heads”, *Trans.ASME*, vol.123, pp. 439-448, Sep (2001).
[6] Peng, J.P. and Harwood, R.F., “Modeling of a General Crown Shape and the Effects on Air Bearing Stedy-State Performance”, *IEEE Trans. Magn*., 32 (5), pp. 3711-3713, Sep (1996).
[7] Philip D. Harvey, “Engineering Properties of Steels”, *American Society for Metals, Metals Park*, OH, (1982).
[8] Zhang, M., Hor, Y.S., Han, G. and Liu, B., “Slider Curvature Adjustment Through Stress Control”, *IEEE Trans. Magn*., 38 (5), pp. 2162-2164, Sep (2002).

FIGURES AND TABLES

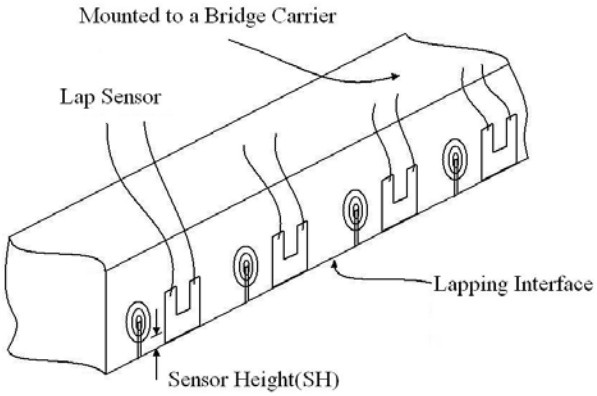

Fig. 1 Slider Bar and Sensor Height (SH).

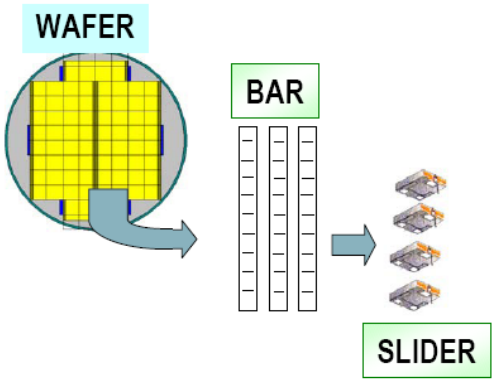

Fig. 2. Wafer to Bar and Slider.

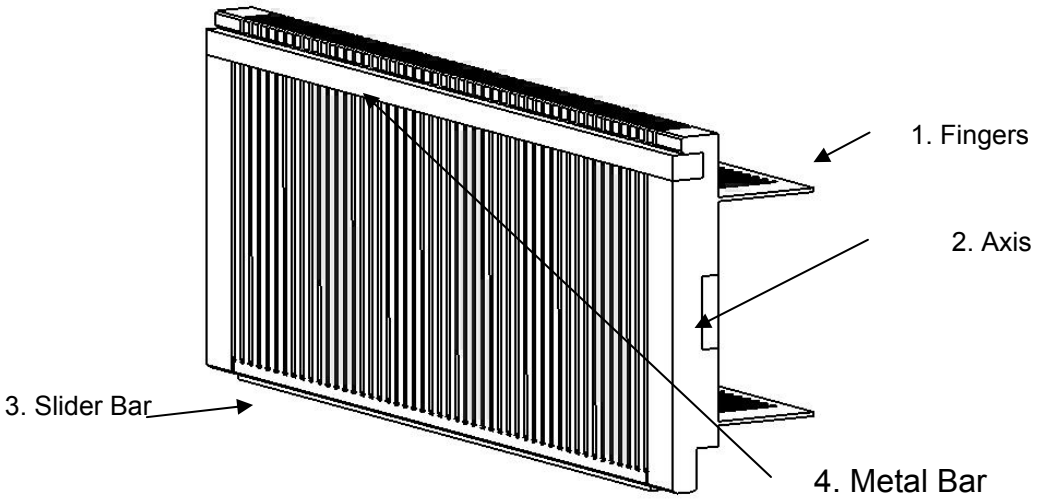

Fig.3. Bridge Carrier Structure.

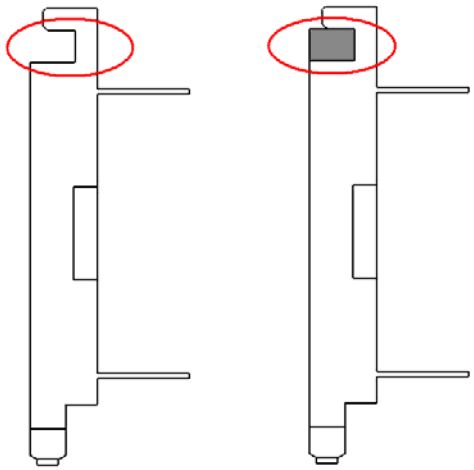

Fig. 4. A Standard Model of Finger (left) and A Model with Metal Bar (right).

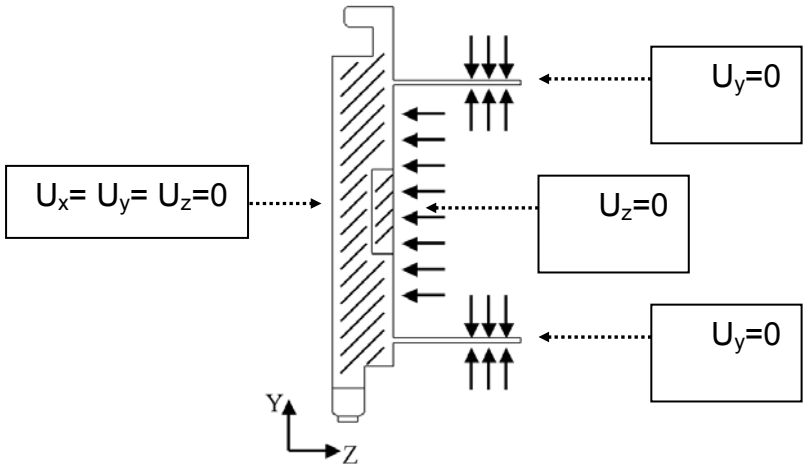

Fig. 5. Zero Degree of Freedom at the Surface

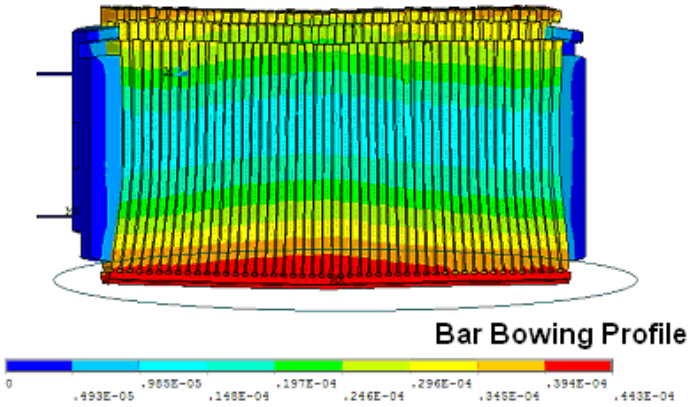

Fig. 6. Deformation of Finger before Improvement.

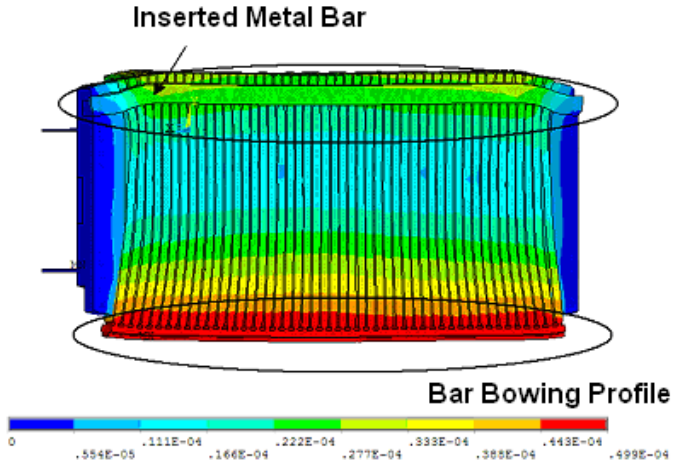

Fig. 7. Deformation of Finger after Improvement.

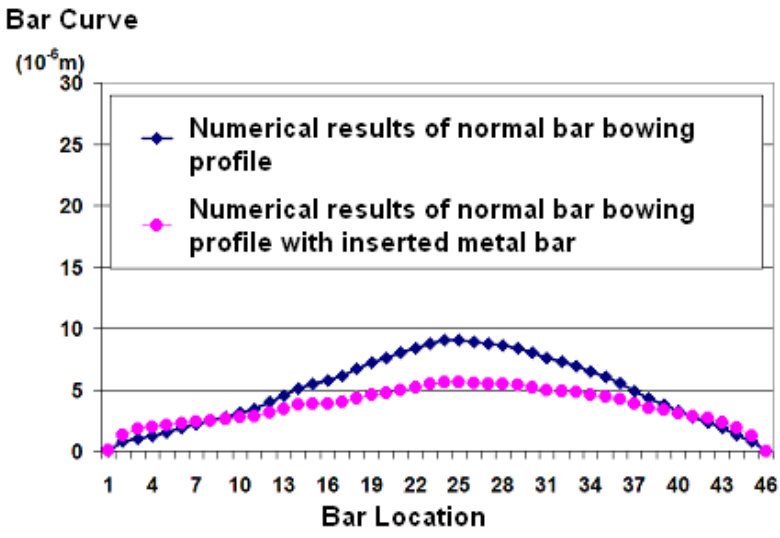

Fig. 8. Bar Bowing Comparison when Heated.

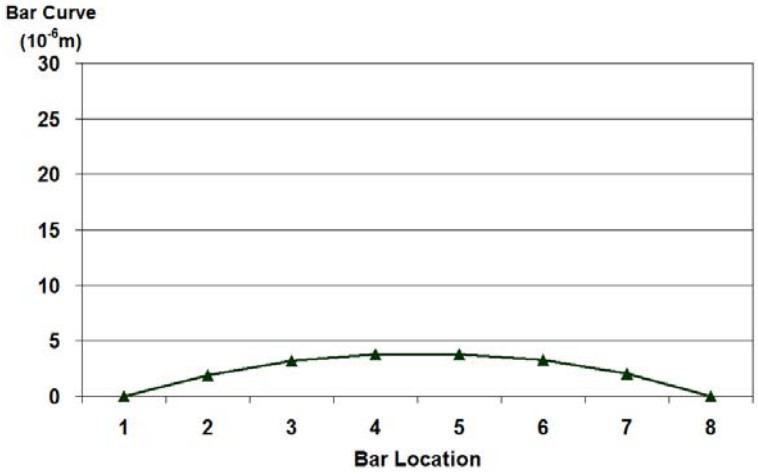

Fig. 9. Bar Curve from Bar Bow Machine.

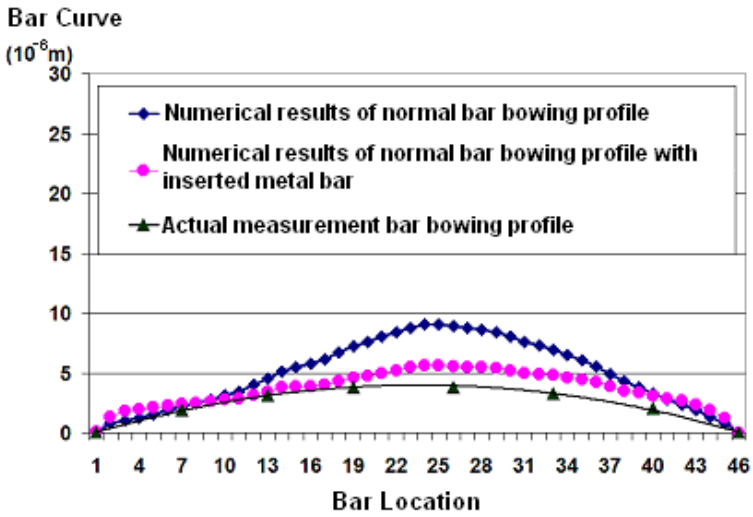

Fig.10. FEM Results and Actual Measurements.

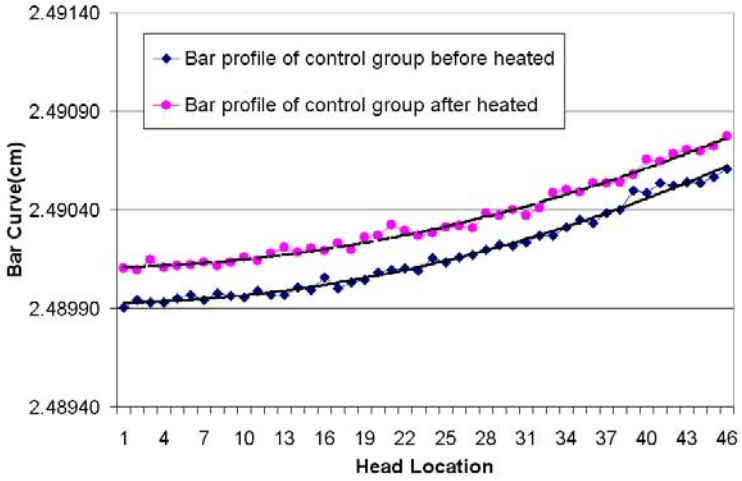

Fig. 11. Bar Control before and after Heated.

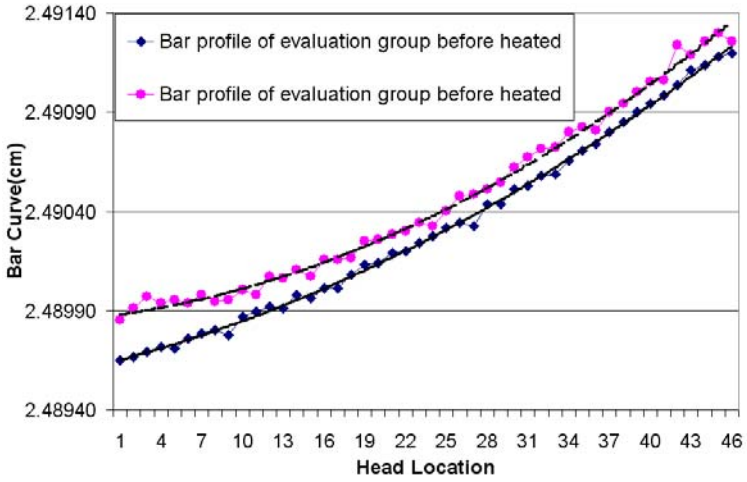

Fig. 12. Bar Evaluation before and after Heated.

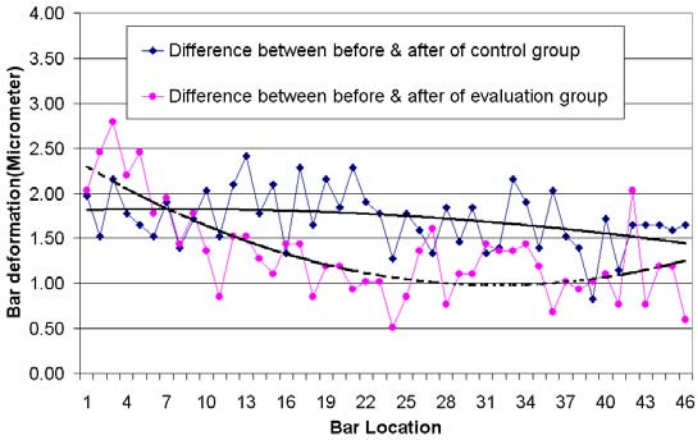

Fig. 13 Bar Deformation of Bar Control and Bar Evaluation.

Table 1. Material properties of a finger.

Properties\Part	1	2	3	4
Modulus of Elasticity (GPa)	200	200	390	193
Poisson's Ratio	0.3	0.3	0.3	0.25
Coefficient Thermal Expansion (10^{-6}/K)	11.3	11.3	7.5	17.8